Signatures of mesoscopic Jahn–Teller polaron inhomogeneities in high-temperature superconductors

2003 J. Phys.: Condens. Matter 15 L169

(http://iopscience.iop.org/0953-8984/15/9/101)

INSTITUTE OF PHYSICS PUBLISHING JOURNAL OF PHYSICS: CONDENSED MATTER

J. Phys.: Condens. Matter **15** (2003) L169–L175 PII: S0953-8984(03)57618-4

LETTER TO THE EDITOR

Signatures of mesoscopic Jahn–Teller polaron inhomogeneities in high-temperature superconductors

A R Bishop[1], **D Mihailovic**[2] **and J Mustre de León**[3]

[1] Theoretical División, Los Alamos National Laboratory, Los Alamos, NM 87545, USA
[2] Institut Jozef Stefan, Jamova 39, 1000, Ljubljana, Slovenia
[3] Deparatemento de Física Aplicada, Cinvestav-Mérida, AP 73, Mérida, Yucatán, 97310, Mexico

Received 18 December 2002
Published 24 February 2003
Online at stacks.iop.org/JPhysCM/15/L169

Abstract

We analyse complementary experimental results in high-temperature superconducting cuprates from x-ray absorption fine structure (XAFS), inelastic neutron scattering (INS) and inelastic x-ray scattering (IXS), Raman spectroscopy (RS), infrared absorption spectroscopy and femtosecond optical spectroscopy in terms of the predictions of a specific fully quantum mechanical calculation of small polaron formation and internal dynamics (phonon-assisted local charge oscillations). These analyses support the scenario in which the pseudogap-associated temperature, T^*, marks the onset of an inhomogeneous ground state with polarons, in agreement with several theoretical models which attempt to explain the origin of high-temperature superconductivity in doped cuprates. The change in dynamics, which is observed across the superconducting transition temperature, T_c in XAFS, INS and RS, indicates an intimate link of the dynamics of these polarons with the mechanism of high-temperature superconductivity.

1. Introduction

During the last decade results from x-ray absorption fine structure (XAFS), inelastic neutron scattering (INS) and inelastic x-ray scattering (IXS), Raman spectroscopy (RS), infrared absorption spectroscopy (IR) and time resolved optical spectroscopy [1–9] have suggested the onset of an inhomogeneous ground state for the doped cuprates as a precursor to the superconducting phase. Manifestations of this inhomogeneity include local lattice distortions, the appearance of anomalous vibrational modes and anomalous isotopic effects, among others. Also, during this period, theoretical models have been developed to explain the appearance of this inhomogeneous ground state and its relation to high-temperature superconductivity [10, 12, 13]. Such models implicitly include the appearance of polaronic behaviour. In this letter we connect experimental results from the techniques mentioned above with the predictions of quantum mechanical calculations of small polaron formation and

internal dynamics (phonon-assisted local charge oscillations) [14]. This comparison supports the scenario in high-T_c cuprates that, T^*, the so-called pseudogap temperature, marks the onset of polaronic formation [12]. We also review XAFS, INS and RS [2–8], which indicate a change in the dynamics of these polarons across the superconducting transition temperature, T_c, suggesting their relation to the mechanism of high-temperature superconductivity, either directly or parasitically.

In the theoretical models referred to above, the polarons have the form of small Jahn–Teller (JT) polarons, which involve coupling of specific in-plane and axial copper–oxygen vibrations to charge carriers. Below T^* the individual polarons become thermally stable, forming a polaron liquid of filamentary segments with at most a very slow polaronic diffusion, but with a much faster internal charge tunnelling accompanied by dynamic lattice distortions. Such tunnelling is a fundamentally quantum mechanical effect. When treated fully nonadiabatically, it leads to an internal dynamical symmetry breaking, which has several measurable manifestations. This phenomenon, also present in other organic and inorganic systems, may be termed variously as internal polaron dynamics [14], local charged phonons [15], local charged breathers [16] or local lattice-assisted dynamic charge transfer [17]. Predicted consequences of the existence of small JT polarons have been observed by optical spectroscopy [6, 7], XAFS [1, 2, 8, 9], pair distribution function analysis of neutron diffraction [18], INS [3, 4] and IXS [5]. The data currently available and discussed here are evidence for small polarons and do not distinguish isolated polarons from their anticipated organization into filamentary segments for $T^* > T > T_c$ as precursors to correlated percolation paths for $T < T_c$.

2. Polaron model and experimental data

An explicit model, which represents these small JT polarons, is given by the Hamiltonian

$$H = H_{el} + H_{ph} + H_{e-ph} \tag{1}$$

$$H_{el} = \sum_i \varepsilon_i n_i + U \sum_i n_{i\uparrow} n_{i\downarrow} + t(c_i^+ c_{i+1} + \text{h.c.}) \tag{1a}$$

$$H_{ph} = \hbar\omega_{IR}^0 b_{IR}^+ b_{IR} + \hbar\omega_R^0 b_R^+ b_R \tag{1b}$$

$$H_{el-ph} = \lambda_{IR}(n_3 - n_1)(b_{IR} + b_{IR}^+) + \lambda_R(n_3 + n_1)(b_R - b_R^+). \tag{1c}$$

This model, originally introduced in [14], is defined over a CuO_2 three-site cluster. Here, $n_{i\sigma} = c_{i\sigma}^+ c_{i\sigma}$ denotes the number operator for holes of spin σ at site i, with site energies ε_i, hopping amplitude t and onsite repulsion U. The phonon part of the Hamiltonian (1b) consists of harmonic Raman and infrared oscillators with creation operators b_R^+ and b_{IR}^+ and bare frequencies ω_R^0, ω_{IR}^0, respectively. The interaction linear term (1c), with coupling constants λ_{IR} and λ_R, reflects the fact that, for holes added at either of the extreme sites, the associated Cu–O bond lengthens and its neighbouring one shortens. We note that the coupling of local half-breathing in-plane [4] and local c-axis modes [9], allowed by local buckling of the CuO_2 planes, defines composite 'ab–c' models [10, 11] and more specific charge transfer centres. Hence, equation (1) should be viewed as a simplification, which allows us to readily obtain exact numerical diagonalization nonadiabatical quantum mechanical results. Manifestations of the polaronic behaviour, derived from this model, include: the appearance of a dynamical lattice distortion, the concomitant existence of an internal 'polaron (charge) tunnelling frequency', ω_T, symmetry forbidden local lattice vibrations (shape modes) [19], anomalous shifts of the

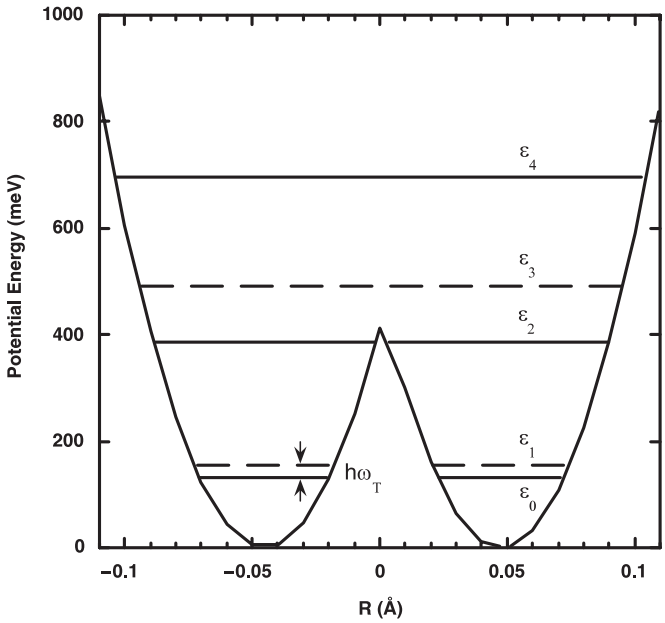

Figure 1. Two-site (double-well) nonlinear potential derived from fits of model (equation (1)) to the copper–in-plane oxygen XAFS signal in $La_2CuO_{4.1}$ [2].

excitation energies under isotopic substitution [14, 20, 21] and strongly enhanced oscillator strengths for specific lattice vibrations [24–26]. None of these properties are assignable by linear phonon analysis, due to the inherent nonlinear and nonadiabatic lattice dynamics arising from the coupling of charge and lattice degrees of freedom in the small polaron.

We identify the polaronic tunnelling frequency as $\omega_T = (\varepsilon_1 - \varepsilon_0)/\hbar$, where ε_0 and ε_1 are, respectively, the ground state and first excited state energies of the many-body Hamiltonian given by equation (1). In the strong coupling limit, in which the charge transfer becomes slow compared to the bare phonon frequencies (i.e. the antiadiabatic limit $\sim$ local ferroelectric dipoles), the ionic dynamics is well described by coherent harmonic oscillator states with specific displaced equilibrium positions. In this limit, the ionic dynamics can be calculated using a *static* double well potential composed of two shifted parabolas (figure 1) [14]. The use of this static double well potential has been useful in the interpretation of XAFS results [1, 2, 8]. However, the use of such a potential leads to an inadequate description of the excited states of the system, leading to errors in the interpretation of spectroscopic data and predictions of the isotopic shifts of the excited state energies, etc [21]. In the model of equation (1), when λ_{IR} is decreased ω_T increases and the charge motion decouples from the ionic motion, resulting in a single-site Cu–O bond distribution. Therefore, we associate the value of ω_T for which we have a single-site distribution instead of the two-site distribution, with the value of the tunnelling frequency when the pseudogap disappears, i.e. disappearance of polarons. From the model equation (1), for $\lambda_{IR} \sim 0.9$ eV one observes a single-peak distribution, with $\hbar\omega_T \sim 30$ meV [14]. This value is essentially confirmed by the results of XAFS experiments, $\hbar\omega_T(T^*) \sim 35$ meV [2], and ultrafast optical probes, which yield a value of the pseudogap energy $\Delta \sim 33$ eV [21]. We note that both of these techniques involve very fast timescale processes, compared to the internal polaron dynamics. Other slower timescale techniques can yield different signatures because they mix the internal and centre of mass JT polaron dynamics, and because they probe spin and charge timescales separately [23]. Correspondingly, the value

Table 1. Energies and average bare phonon numbers of the many-body states derived from the Hamiltonian described by equation (1) (parameter values given in the text).

State	Energy (meV)	$\langle N_{IR}\rangle$	$\langle N_R\rangle$	Character of excitation
0	0	0.9	0.1	Ground state
1	12	1.9	0.1	IR
2	49	2.4	0.1	Raman
3	62	0.9	1.0	Raman
4	74	1.9	1.1	IR
6	84	3.5	0.1	IR
7	111	2.4	1.1	Overtone of state 2
8	124	0.9	2.0	Overtone of state 3

of T^* depends on the timescale of the probe employed. In table 1 we report the results for the ground state and first few excitations obtained from the exact numerical diagonalization of equation (1), with: $U = 7$ eV, $t = 0.5$ eV, $\varepsilon_{1,3} = 0.5$ eV, $\varepsilon_2 = -0.5$ eV [14]. For the bare phonon energies we have taken the observed experimental values for $YBa_2Cu_3O_7$, above T^*, $\hbar\omega_R^0 = 62$ meV [7] and $\hbar\omega_{IR}^0 = 73$ meV [24]. We selected $\lambda_{IR} = 0.128$ eV, which leads to a double-peaked radial distribution function for the Cu–O bond with a separation of 0.11 Å, consistent with the XAFS results in $YBa_2Cu_3O_7$ and other cuprates [1, 2, 8, 9]. The effect of λ_R is to modify the average Cu–O bond length. Since no change is observed across T^* (when the polaron is formed), we have chosen $\lambda_R = 0.03$ eV, which yields a negligible change of this bond length. (Previous calculations [14] yielded a large change in the average Cu–O distance accompanied by a strong renormalization of the Raman frequencies.) In the coupling regime discussed the numbers of bare phonons are no longer good quantum numbers. In this sense all excitations are multiphonon excitations. However, for some of them the fluctuations with respect to the average number of phonons are small, making the labelling of a given excitation in terms of the average number of Raman and IR quanta still useful. The first excitation of the many-body system (equation (1)) at 12 meV corresponds to the polaron tunnelling and is an IR-active mode. The next two excitations at 49 and 62 meV are Raman-active excitations. The 49 meV excitation is a nonlinear multiphonon excitation, while the 62 meV excitation corresponds to the weakly renormalized bare Raman mode. The next two excitations at 74 and 84 meV are infrared-active. The 74 meV excitation corresponds to a state with approximately one IR and one Raman phonon above the ground state. The 84 meV excitation corresponds to a state described by approximately 3.5 infrared-active bare phonons and, in the limit of very strong coupling, would converge to the value of a harmonic bare IR phonon (but the oscillator would have a displaced equilibrium position). At higher energies, Raman-active excitations appear as overtones of the 49 and 62 meV excitations in intervals of $\sim$62 meV.

The multiphonon excitations described above were either not observed in direct infrared or Raman measurements, or misassigned, because the local nature of the JT polarons implies projection into multiple linear q modes. INS results are especially important in this regard. In [3] modes at wavevector (q)-57 and 87 meV modes are present, which were not consistent with previous infrared and Raman assignments [3]. We identify these peaks with the 49 and 84 meV multiphonon excitations predicted in our present calculation. In [3] it was also found that the integrated intensity in the 57–65 meV region shows anomalies across the superconducting transition with specific low-symmetry wavevectors (i.e. away from the zone boundaries), implying a length scale $\sim$6 Å [3]. This length scale defines the polaron size. The crossover of the mode at 85 meV at $q = 0$ to the mode at 70 meV at $q = \pi$, observed in $La_{1.85}Sr_{0.15}CuO_4$ at low temperatures [4], can be interpreted as evidence of polaronic

tunnelling, with the energy difference $\Delta\varepsilon = 15$ meV corresponding to the polaron tunnelling energy $\hbar\omega_T$ (12 meV in our simplified calculation).

Another experimental observation which supports the presence of polaronic objects below T^* is the isotope effect on T^*, observed by INS [23]. We note that, under oxygen isotope substitution, $T^*(O_{18}) > T^*(O_{16})$, with a shift $\sim$30%. Such a shift is notably opposite to the shift of the frequencies of harmonic phonons, which *soften* under such substitution. However, ω_T presents the same behaviour as T^* (i.e. $\omega_T(O_{18}) > \omega_T(O_{16})$) with a calculated shift of 9% [21]. This behaviour suggests a direct relation between the energy of formation of the JT polarons ($k_B T^*$) with the energy scale of their internal dynamics ($\hbar\omega_T$), supporting the identification of $\omega_T(T^*)$ as the timescale associated with the pseudogap disappearance.

The appearance of an inhomogeneous ground state below T^*, with a polaronic character, must also give rise to *accompanying* changes in the optical region, particularly in the range of interband or charge transfer transitions ($\sim$1.5 eV). In our model, this region corresponds to transitions between the ground state and free-electron-like levels, which are also not described adequately by a rigid potential model. A change in the region around 1.5 eV has indeed been observed in the vicinity of T_c in a number of optimally doped cuprates [27]. This change can be interpreted as a consequence of the nonlinear excitations discussed above, since the ground state of the system (and its excitations) has a different character below T^*.

Below T^* the polaron liquid begins to condense and, due to combinations of short range (lattice scale) and long-range (Coulomb and elastic) forces, forms mesoscopic patterns of clumps and filamentary stripe segments. These objects are predicted to exhibit correlated, dynamic percolation at around 6% doping and they persist at least to optimal doping, where changes of the ground state should occur because of the quantum melting of overlapping polarons [22]. In this phase there is presumably a coexistence of these objects as well as unbound fermions. Whether these mesoscopic formations are the regions in which superconductivity exist, and if they coexist with the individual JT polarons, is still a matter of debate [22]. Consequently, experimental information that shows a relation between the JT polarons and the superconducting transition is important. In figure 2 we show the temperature behaviour of ω_T for the optimally doped systems $La_2CuO_{4.1}$ ($T_c = 41$ K), $Tl_2Ba_2CuO_6$ ($T_c = 89$ K), $Tl_2CaBa_2Cu_2O_8$ ($T_c = 105$ K) and overdoped $Tl_2Ba_{1.2}Sr_{0.8}CuO_6$ ($T_c = 57$ K) obtained from XAFS measurements [2, 8]. This figure shows, for all these superconducting compounds, an anomalous behaviour of ω_T in the vicinity of T_c, establishing that the polaronic dynamics is, at the very least, affected by the superconducting transition. It is interesting to note the contrasting behaviour of ω_T in the vicinity of T_c for the overdoped material, where individual polarons are expected to lose their identities. Behaviour similar to the ω_T anomaly around T_c is shown by the integrated INS structure factor in the energy region corresponding to Cu–O stretching bonds in $YBa_2Cu_3O_7$ (figure 5 in [3]) and in the widths of the peaks associated with the two highest energy Cu–O modes in $Bi_2Sr_2CaCu_2O_8$ [28]. Also, RS measurements show a sharp decrease in the intensity of the Ba mode of $YBa_2Cu_3O_7$ and an increase of other modes across T_c (or T^*), given the proximity of these two temperatures near optimal doping and the resolution of the temperature grid available in the experiments, figure 7 in [7]). While the data reviewed here cannot specify the superconductivity mechanism onset at $T_c (< T^*)$, the anomaly in the polaronic signatures, found by XAFS [2, 8] (figure 2), RS [7] and INS [3, 28], minimally demonstrate a coupling between the charged particles involved in pairing and the polarons. In this regard, it is important to note that recent photoemission studies have reported an anomaly in the quasi-particle dispersion curve with the same q vector as the INS results of [4], suggesting a common origin for both anomalies [29].

A local 'Ising' symmetry, which is consistent with the ab–c coupling from c-axis buckling, is especially helpful for pairing [10]. The ab–c coupling supports an appealing two-band

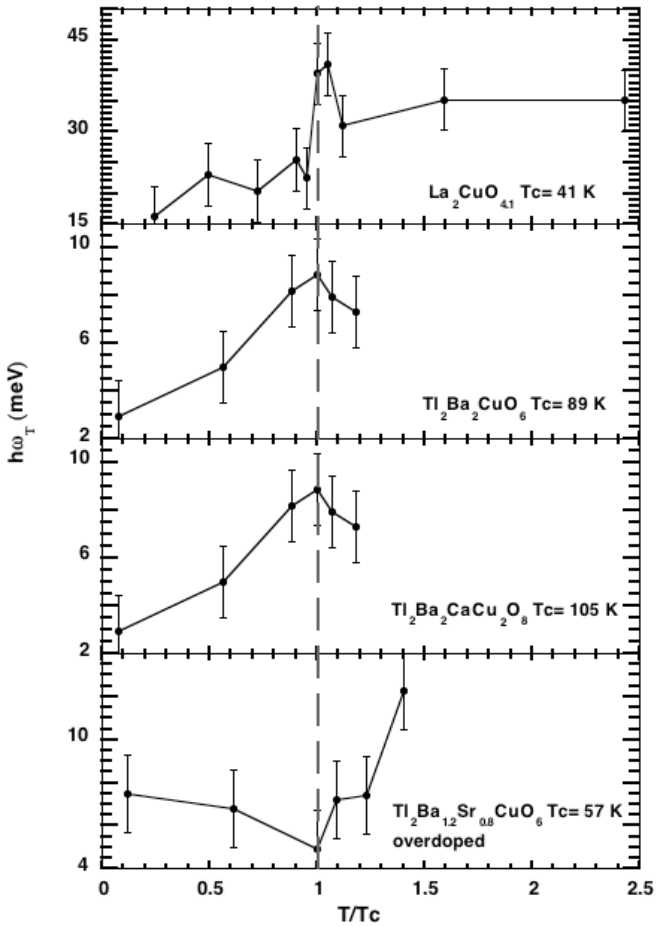

Figure 2. Energy associated with internal polaron tunnelling, $\hbar\omega_T$, as a function of temperature (T/T_c) extracted from XAFS measurements on $La_2CuO_{4.1}$ ($T_c = 41$ K) [2], $Tl_2Ba_2CuO_6$ ($T_c = 89$ K) [8], $Tl_2CaBa_2Cu_2O_8$ ($T_c = 105$ K) [8] and overdoped $Tl_2Ba_{1.2}Sr_{0.8}CuO_6$ ($T_c = 57$ K) [8]. Error bars were estimated using the measurement with the largest error bar.

(This figure is in colour only in the electronic version)

model coupling ferroelectric and magnetic channels to produce superconductivity [10, 11]. Inhomogeneous percolation or Josephson junction coupling may be relevant below optimal doping while a homogeneous Bose condensation or a BCS-like mechanism can be important above optimal doping [12].

Finally, we note that the two-site distribution with low tunnelling frequency *below* T_c, obtained from XAFS [2, 8], supports the *coexistence* of charge carriers and their associated polaronic dynamic distortions with superconductivity, implied by several independent experiments [21].

3. Conclusions

Correlating data from XAFS, INS and optical spectroscopies with specific small JT polaron (nonlinear and nonadiabatic) model predictions reveals a rich phenomenology of local lattice

distortions, symmetry forbidden vibrational modes, and anomalous isotope effects. The substantial semi-quantitative consistency among all the different data analysed here strongly suggests the need for new, more extensive systematic experimental studies, which can be compared quantitatively with theoretical predictions, and hopefully revealing the detailed connection between these effects and superconductivity in cuprates.

We acknowledge illuminating discussions with P Calvani and V Kabanov. This work was supported in part by the US Department of Energy and by CONACYT-Mexico.

References

[1] Mustre de Leon J, Conradson S D, Batistic I and Bishop A R 1990 *Phys. Rev. Lett.* **65** 1675
[2] Acosta-Alejandro M, Mustre de Leon J, Conradson S D and Bishop A R 2002 *J. Supercond.* **15** 355
[3] Arai M *et al* 1992 *Phys. Rev. Lett.* **69** 359
[4] McQueeney R J *et al* 1999 *Phys. Rev. Lett.* **82** 628
[5] D' Astuto M *et al* 2002 *Phys. Rev. Lett.* **88** 167002
[6] Demsar J *et al* 1999 *Phys. Rev. Lett.* **82** 4918
[7] Misochko O V *et al* 1999 *Phys. Rev.* B **59** 11495
[8] Mustre de Leon J *et al* 1994 *Physica* C **220** 377
[9] Bianconi A *et al* 1996 *Phys. Rev. Lett.* **76** 3412
Saini N L *et al* 1997 *Phys. Rev.* B **55** 12759
[10] Bussman-Holder A *et al* 2001 *J. Phys.: Condens. Matter* **13** L545
[11] Shenoy S R, Subrahmanyam V and Bishop A R 1997 *Phys. Rev. Lett.* **79** 4657
[12] Mihailovic D and Kabanov V V 2001 *Phys. Rev.* B **63** 054505
Kabanov V V and Mihailovic D 2000 *Phys. Rev.* B **61** 2125
[13] Ovchinnikov Y N, Wolf S A and Kresin V Z 2001 *Phys. Rev.* B **63** 064524
[14] Mustre de Leon J, Batistic I, Bishop A R, Conradson S D and Trugman S A 1992 *Phys. Rev. Lett.* **68** 3236
[15] Rice M J and Choi H-Y 1992 *Phys. Rev.* B **45** 10173
Friedman B 1993 *Phys. Rev.* B **48** 17551
[16] Aubrey S 1994 *Physica* D **71** 196
[17] Hennessy M H, Zoos Z G, Pascal R A and Girlando A 1999 *Chem. Phys.* **245** 199
[18] Bozin E S, Kwei G H, Takagi H and Billinge S J L *Phys. Rev. Lett.* **84** 5856
[19] Mihailovic D *et al* 1991 *Phys. Rev.* B **44** 237
[20] Salkola M, Mustre de Leon J, Trugman S A and Bishop A R 1994 *Phys. Rev.* B **49** 3671
[21] Mustre de Leon J, De Coss R, Bishop A R and Trugman S A 1999 *Phys. Rev.* B **59** 8359
[22] Kabanov V V and Mihalovic D 2002 *Phys. Rev.* B **65** 212508
Mihalovic D, Kabanov V V and Muller K A 2002 *Eur. Phys. Lett.* **57** 254
Mihalovic D, Kabanov V V and Muller K A 1999 *Phys. Rev.* B **60** R6995
[23] Rubio Temprano D *et al* 2000 *Phys. Rev. Lett.* **84** 1990
[24] Genzel L *et al* 1989 *Phys. Rev.* B **40** 2170
[25] Bernhard C *et al* 2002 unpublished
[26] Batistic I, Bishop A R, Martin R and Tesanovic Z 1989 *Phys. Rev.* B **40** 6896
[27] Holcomb L J and Little W A 2000 *Physica* C **341** 2223
Stevens C J *et al* 1996 *Phys. Rev. Lett.* **78** 2212
[28] Mook H A *et al* 1992 *Phys. Rev. Lett.* **69** 2272
[29] Lanzara A *et al* 2001 *Nature* **412** 510